

Domain Generalization via Frequency-based Feature Disentanglement and Interaction

Jingye Wang, Ruoyi Du, Dongliang Chang and Zhanyu Ma*

Pattern Recognition and Intelligent Systems Lab., Beijing University of Posts and Telecommunications, Beijing

Abstract

Data out-of-distribution is a meta-challenge for all statistical learning algorithms that strongly rely on the i.i.d. assumption. It leads to unavoidable labor costs and confidence crises in realistic applications. For that, domain generalization aims at mining domain-irrelevant knowledge from multiple source domains that can generalize to unseen target domains with unknown distributions. In this paper, leveraging the image frequency domain, we uniquely work with two key observations: (i) the high-frequency information of images depict object edge structure, which is naturally consistent across different domains, and (ii) the low-frequency component retains object smooth structure but are much more domain-specific. Motivated by these insights, we introduce (i) an encoder-decoder structure for high-frequency and low-frequency feature disentangling, (ii) an information interaction mechanism that ensures helpful knowledge from both two parts can cooperate effectively, and (iii) a novel data augmentation technique that works on the frequency domain for encouraging robustness of the network. The proposed method obtains state-of-the-art results on three widely used domain generalization benchmarks (Digit-DG, Office-Home, and PACS).

1 Introduction

With the development of deep learning methods, it plays an increasingly important role in various fields of computer vision, which relies on the i.i.d. assumption. However, the distribution of training data and test data often encounter significant shifts in practical applications (e.g., recognizing the same object in cartoons and art paintings), which may lead to sharp performance degradation of the deep neural network. Domain adaption (DA) and domain generalization (DG) were proposed to solve this problem. However, DA requires labeled or unlabeled data from the source domain to conduct the model adaptation, which makes it less practical in realistic scenarios compared with DG. Specifically, DG aims at training the model with multiple source domains so that it

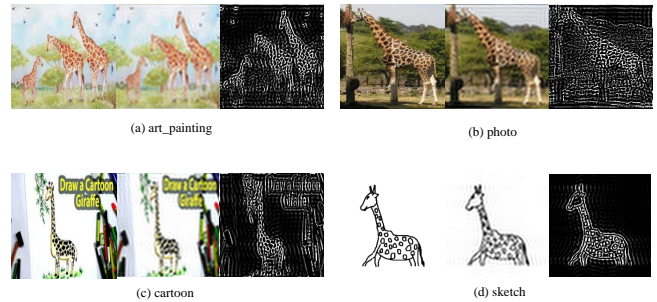


Figure 1: Examples of the same category in four domains from PACS dataset. We can see that the high-pass filtered versions retain the edge features of the object, which is less affected by the domain shift. And low-pass filtered versions retain image smooth contour information, which can assist high-frequency information for classification.

can be generalized to target domains with unknown distributions. The existing DG methods can roughly divided into three directions [Wang *et al.*, 2021]: data manipulation [Zhou *et al.*, 2020b; Li *et al.*, 2021; Zhou *et al.*, 2021], representation learning [Wang *et al.*, 2020b; Li *et al.*, 2018; Matsuura and Harada, 2020], and learning strategy [Li *et al.*, 2019; Carlucci *et al.*, 2019].

Nevertheless, these previous arts mainly focus on how to learn with inter-domain interpolation or mine domain-irrelevant knowledge, but less or no efforts are paid for investigating the very question that which components of images carry the discriminative information shared across domains. In this paper, instead of leaving everything to the model to learn, we tackle domain generalization problems with an empirical prior knowledge. In particular, we uniquely work with image frequency domain under two observations: (i) the high-frequency information of images depict object edge structure, which is naturally consistent across different domains [Xu *et al.*, 2021], and (ii) the low-frequency component contains object smooth structure that retains more energy distributions of images but is much more domain-specific [Yang and Soatto, 2020]. To better understand this idea, we perform the Fast Fourier Transform (FFT) on several images of the same category from four domains to obtain their high-pass filtered versions and low-pass filtered versions. As shown in Figure 1, we can easily find that the high-pass filtered images of the

*Corresponding author

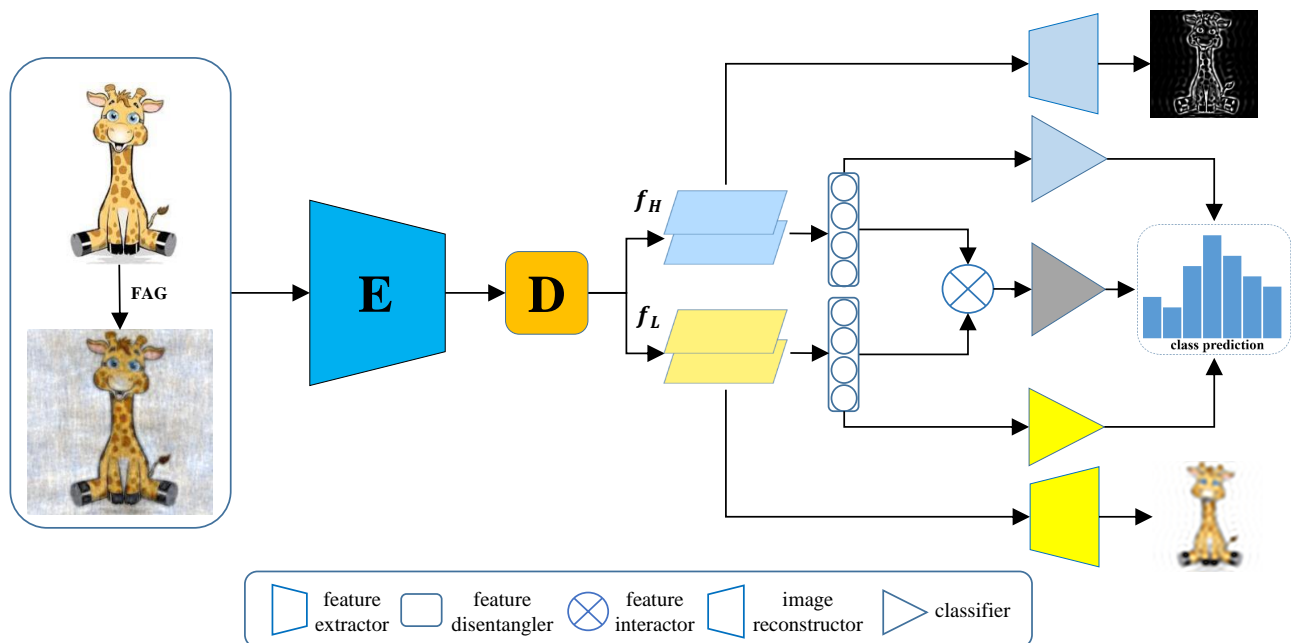


Figure 2: The architecture of the proposed FFDI. We employ frequency disentanglement to disentangle corresponding high- or low-frequency features. Then we interact between the disentangled frequency-specific features by using bilinear pooling. Furthermore, we propose a simple frequency-domain-based data augmentation(FAG) to strengthen the robustness of the network.

giraffes from four different domains are less affected by the domain shifts. However, high-pass filtered images indicate where the gray value changes on a large scale [Juneja and Sandhu, 2009] but lose most of the energies of the images, which makes them more likely to be affected by noises caused by background edge structures (*i.e.*, making it hard to distinguish the foreground and the background). On the contrary, although low-pass filtered images are much more domain-specific, they still retain most of the image energies, (*i.e.*, retaining the object location information). Hence, we argue that low-frequency information can be complementary to high-frequency information and assist with high-frequency information while performing recognition. Taking Figure 1(b) as an example, it is difficult to distinguish the giraffe in the woods by high-pass filtered image, and low-pass filtered image can assist us to alleviate the impact of background.

To realize the above idea, we introduce a Frequency-based Feature Disentanglement and Interaction (FFDI) framework, which consists of three modules: encoder-decoder structure, information interaction mechanism, and frequency-domain-based data augmentation (FAG), as shown in Figure. 2. First of all, we construct an encoder-decoder structure, which uses the idea of disentanglement [Peng *et al.*, 2019] to obtain the high- and low-frequency features of the image. Second, we hope to perform the interaction between high-frequency features and low-frequency features to improve the representation ability of the network. Intuitively, we use bilinear pooling [Lin *et al.*, 2015] to do this. Bilinear pooling structure is related to the dual-stream hypothesis of visual processing in the human brain, which has two main pathways, or "streams": the ventral stream (or "what pathway") is involved with semantic information, and the dorsal stream (or "where

pathway") involves spatial location information. We argue that the bilinear pooling structure can effectively combine the helpful information in the high- and low-frequency features of the image. Finally, to further improve the robustness of the network, inspired by many recent works that aim to solve the domain shifts problem based on frequency domain [Yang and Soatto, 2020; Xu *et al.*, 2021], we proposed a simple frequency-domain-based data augmentation.

The contributions of our work are summarized as follow:

- We propose a new network structure named FFDI that can disentangle high- and low-frequency features of the image, and then fuse them by using bilinear pooling to improve the representation ability of the model.
- According to the respective characteristics of high- and low-frequency images, we propose a simple data augmentation method based on frequency domain, which can enhance the diversity of the sample data distribution.
- We demonstrate the effectiveness of our idea on three standard domain generalization benchmarks, Digit-DG, Office-Home, and PACS, which shows our method achieves state-of-the-art results.

2 Related Work

Domain Generalization: In recent years, various DG methods have been proposed to solve the domain shifts problem. [Li *et al.*, 2021] proposes a data augmentation method for feature embedding during training, which can be combined with some existing methods to obtain better generalization performance. [Wang *et al.*, 2020b] proposes EIS-Net that used extrinsic relationship supervision and intrinsic

self-supervision for images to implement domain generalization. [Li *et al.*, 2019] proposes an episodic learning strategy to obtain a robust baseline. [Matsuura and Harada, 2020] uses clustering and adversarial learning to obtain domain invariant features, which does not use domain labels.

Our work is relevant to the frequency-domain-based DG methods. Inspired by some DA algorithms [Yang and Soatto, 2020; Yang *et al.*, 2020], [Xu *et al.*, 2021] argues that the phase information of images contains high-level semantic information and develop a Fourier-based data augmentation strategy by mixing the amplitude parts of two images aims to force the model to capture phase information. [Huang *et al.*, 2021] improves the generalization of the network by keeping the domain invariant frequency components and randomizing the domain variant frequency components. Different from previous algorithms, in this paper, we disentangle the high- and low-frequency features in the latent feature space and interact between them to obtain more generalized features.

Representation Disentanglement: Representation disentanglement is an active research topic in the field of computer vision. In face recognition, [Wang *et al.*, 2020a] proposes to disentangle PAD informative features and subject discriminative features by using a pair of encoders which is learned by generative models. In image translation, [Gonzalez-Garcia *et al.*, 2018] extracts content space and style space from latent space of the image. Aims to improve the generalization capabilities, [Sanchez *et al.*, 2020] captures a shared representation and an exclusive representation information of each image by mutual information estimation. [Yang *et al.*, 2019] proposes a unified network structure named M^2RD to learn domain-invariant content representations and related domain-specific representations. [Peng *et al.*, 2019] design a deep adversarial disentangled auto-encoder ($DADA$) to disentangle domain-specific features from class identity. In this paper, We disentangle the high- and low-frequency of the image in the latent space by using an encoder-decoder structure.

3 Methodology

We define the domain generalization task as follows: Given K source domains $D_S = \{D_1, \dots, D_K\}$ as the training set, with the i -th domain D_i having N_i sample pairs $\{(x_j^i, y_j^i)\}_{j=1}^{N_i}$, where (x_j^i, y_j^i) is the j -th sample pair in D_i . We plan to learn a model from multiple source domains that can be generalized to the unseen target domains D_T with unknown distributions.

In this paper, to solve the problem of network performance degradation caused by domain shifts, we proposed frequency-based feature disentanglement and interaction framework. The overall network structure of our method is shown in Figure. 2. The feature extractor $E(\cdot)$ maps the input image to the feature map f_E . The disentangler $D(\cdot)$ is responsible for disentangling the features f_E into high-frequency features f_H and low-frequency features f_L . The image reconstructor $R(\cdot)$ aims to recover high-pass (or low-pass) filtered images from f_H (or f_L). $D(\cdot)$ and $R(\cdot)$ are implemented as the encoder and decoder in Convolution Auto-Encoders (CAE). To improve the representation ability of the feature, we use

the feature interactor for the fusion of vectors of f_H and f_L . Then we use three classifiers $c_{A_H}(\cdot)$, $c_{A_L}(\cdot)$, $c_I(\cdot)$ corresponding to high-frequency features, low-frequency features, and fused features respectively to predict the class distribution f_C , which is trained on the labeled source domain. Furthermore, we propose a frequency-domain-based data augmentation method, which can enhance the robustness of the network. We next describe each module in detail.

3.1 Frequency Disentanglement

We use CAE to extract high- and low-frequency features of the image. First, we transform each channel of the RGB image I to the frequency domain space by using the Fourier transformation, which is formulated as:

$$F(u, v) = \sum_{a=0}^{A-1} \sum_{b=0}^{B-1} x(a, b) e^{-j2\pi(au/A + bv/B)} \quad (1)$$

We use the symbol $F^{-1}(u, v)$ to denote the inverse Fourier transformation. Further, we denote with M a mask, whose value is zero except for the center region:

$$M = \begin{cases} 1, & (u, v) \in [c_x - r : c_x + r, c_y - r : c_y + r] \\ 0, & \text{others} \end{cases} \quad (2)$$

where (c_x, c_y) denotes the center of the image and r indicates the frequency threshold that distinguishes between high and low frequencies of the original image as shown in Figure. 3. Then, the low-pass filtered image (LFI) and high-pass filtered image (HFI) can be obtained as follows:

$$LFI = F^{-1}(F(u, v) \circ M) \quad (3)$$

$$HFI = I - LFI \quad (4)$$

where \circ denotes the Hadamard product of the matrix. And the obtained LFI and HFI are used as the CAE 's optimization targets. Second, we train the disentangler $D(\cdot)$ and reconstructor $R(\cdot)$ to correctly reconstruct the corresponding HFI and LFI . The reconstruction error of the CAE over all the seen source domains is defined as

$$L_{cae} = \frac{1}{K} \sum_{i=1}^K \frac{1}{N_i} \sum_{j=1}^{N_i} \|X_{f_j} - X'_{f_j}\|_2^2 \quad (5)$$

where $X_f \in \{LFI, HFI\}$, X'_f is the output of $R(\cdot)$.

By using HFI and LFI as target labels for high-pass filtered image and low-pass filtered image reconstruction respectively, we can make the embedded features f_H or f_L more biased towards high-frequency features or low-frequency features of the image.

Finally, we use the extracted vector of frequency-specific features as input to train the auxiliary classifier (c_{A_H} , c_{A_L}) to correctly predict the sample class, which allows the vector of frequency-specific features to obtain corresponding semantic information and speeds up the training of the network. This can be achieved by minimizing the standard cross-entropy loss:

$$L_{ca} = -\frac{1}{K} \sum_{i=1}^K \frac{1}{N_i} \sum_{j=1}^{N_i} y_j^i \log(c_A(\text{vector}(f_{E_j}))) \quad (6)$$

where $f_F \in \{f_H, f_L\}$, $c_A \in \{c_{A_H}, c_{A_L}\}$.

3.2 Interaction of Frequency-specific Features

As analyzed in the Sec. 1, to make full use of the helpful information of both f_H and f_L , we establish an effective interaction mechanism based on them. Inspired by [Lin *et al.*, 2015], we perform the interaction between f_H and f_L using bilinear pooling. In this paper, we design an efficient network structure where the feature extractor is shared in the early stage, then process the corresponding frequency features respectively, and finally interact between disentangled high- and low-frequency features.

To be specific, for features $f_L \in R^{C \times H \times W}$ and $f_H \in R^{C \times H \times W}$ extracted from the same sample, where C, H, W respectively denote the number of channels, height, and width of the feature map, bilinear pooling is used to obtain a fused vector of the two features, which is then used for classification. First, we reshape the matrix dimension: $f_F \in R^{C \times H \times W} \rightarrow f'_F \in R^{C \times (HW)}$. Then compute the matrix outer product at each position of the two features for feature combination, and we aggregate the bilinear features across the image by using sum-pooling, formula is as follows:

$$B(f'_H, f'_L) = \frac{f'_H f'^T_L}{HW} \quad (7)$$

which is equivalent to measuring the cosine similarity of high- and low-frequency features in the spatial dimension. Note that f_H and f_L have the same feature dimension. Then we flattened B to obtain the bilinear vector $b \in R^{C \times C \times 1}$. The fused feature z is obtained by signed squareroot step and l_2 normalization:

$$y = \text{sign}(b) \sqrt{|b|} \quad (8)$$

$$z = \frac{y}{\|y\|_2} \quad (9)$$

After that, we use fused feature z as the input of classifier c_I consisting of a fully connected layer to correctly predict the class of the each image, which is supervised by the cross-entropy loss:

$$L_{ci} = -\frac{1}{K} \sum_{i=1}^K \frac{1}{N_i} \sum_{j=1}^{N_i} y_j^i \log(c_I(z_j)) \quad (10)$$

Intuitively, by jointly training f_H and f_L , the bilinear pooling can effectively trade-off the ability of data-based feature representation. We hope to use the interaction between all feature pairs of f_H and f_L for mutual constraints, which may allow the network to learn object edge features in high-frequency features while also noticing helpful information in low-frequency features.

3.3 Frequency-domain-based Data Augmentation

In order to further enhance the robustness of the network, we propose a simple data augmentation technique that works on the frequency domain. First, we obtain the frequency domain representation of the image using Eq. 1. And then we convert it to polar coordinate form:

$$F(u, v) = |F(u, v)| e^{-j\phi(u, v)} \quad (11)$$

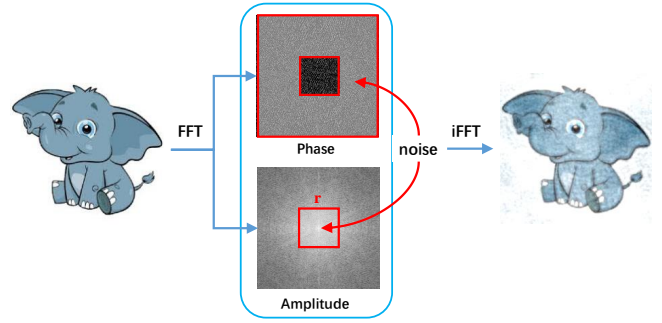


Figure 3: We add noise to the high frequencies of the phase and to the low frequencies of the amplitude. r is the threshold value to distinguish between high and low frequencies.

so that we can obtain the mathematical expressions for its amplitude and phase:

$$A(u, v) = |F(u, v)| \quad (12)$$

$$P(u, v) = \phi(u, v) \quad (13)$$

In this paper, we attempt to use random noise in the frequency domain to augment the image. The high-pass filtered image retains the edge information of the image, which has some similarity with the phase [Xu *et al.*, 2021], so we properly perturb the phase of the high-pass filtered image (P_H) to enhance the robustness of the network in recognizing object edge structures. For the *LFI* that are much more domain-specific, follow [Yang and Soatto, 2020], which exchanges the amplitude information of the source and target domains in the low-frequency part for domain alignment, we generalize them by adding noise directly to the amplitude part of the low-frequency (A_L) to increase the diversity of the low-pass filtered image without applying domain labels. Specifically, inspired by [Li *et al.*, 2021], we add or multiply random variables sampled from a certain distribution over the phase or amplitude. The computation formula is as follows:

$$\hat{A}_g = \alpha \circ A_g + \beta \quad (14)$$

where $A_g \in \{P_H, A_L\}$, $\alpha \in R^{C \times H \times W}$ and $\beta \in R^{C \times H \times W}$ are noise. For example, each element α is sampled from Uniform distributions $U(a, b)$ and β is sampled from Normal distributions $N(\mu, \sigma^2)$. We then feed \hat{A}_g into the inverse Fourier transform to obtain the augmented image. The process of data augmentation proposed in this paper is shown in Figure. 3.

3.4 Algorithm Flow

The above three components together form the FFDI framework. We can use the overall loss L_{all} to train our model in an end-to-end fashion as follow:

$$L_{all} = L_{ci} + \lambda(L_{ca_L} + L_{ca_H} + L_{cae_L} + L_{cae_H}) \quad (15)$$

It is noteworthy that, in practice, when training we first need to pre-process the data: 1) FAG to augment the data; 2) FFT to extract the high- and low-pass filtered image. And then we train the network using Eq. 15. After training, only feature extractor E , disentangler D , and classifiers c_I will be deployed for testing.

4 Experiments

4.1 Datasets and Setting

Datasets: To validate the performance of the proposed method FFDI, we conduct extensive experiments on the following datasets: PACS [Li *et al.*, 2017] that consists of four domains with different data distribution (*Photo*, *Art painting*, *Cartoon*, and *Sketch*) where each domain contains 7 categories, and the whole dataset has 9,991 images. Digits-DG [Zhou *et al.*, 2020b] contains four datasets (*MNITS*, *MNIST-M*, *SVHN*, and *SYN*) in the field of digital handwriting recognition as different domains with diverse image background and style. Following the experimental protocol of [Zhou *et al.*, 2020b], each domain has 600 images per category, and the ratio of the training and test sets in the source domain is 4 : 1. Office-Home [Venkateswara *et al.*, 2017] is composed of four domains (*Art*, *Clipart*, *Product*, and *Real world*) with a total of 15,500 images and 65 categories for each of its domains. This dataset contains images with various styles and viewpoints. Following the setting of [Zhou *et al.*, 2020b], we split the dataset according to training : test = 9 : 1.

Competitors: We evaluate FFDI with the following DG methods: (1) CCSA [Motiian *et al.*, 2017]; (2) CrossGrad [Shankar *et al.*, 2018]; (3) MetaReg [Balaji *et al.*, 2018]; (4) MMD-AAE [Li *et al.*, 2018]; (5) Epi-FCR [Li *et al.*, 2019]; (6) JiGen [Carlucci *et al.*, 2019]; (7) DDAIG [Zhou *et al.*, 2020a]; (8) CSD [Piratla *et al.*, 2020]; (9) L2A-OT [Zhou *et al.*, 2020b]; (10) MixStyle [Zhou *et al.*, 2021]; (11) RSC [Huang *et al.*, 2020]; (12) EISNet [Wang *et al.*, 2020b]; (13) ATSRL [Yang *et al.*, 2021]; (14) MDGH [Mahajan *et al.*, 2021];

Evaluation Protocol: To make a fair comparison, we follow [Zhou *et al.*, 2020b; Venkateswara *et al.*, 2017] to apply the leave-one-domain-out protocol. We select one domain as the unseen domain and the rest of the domains are considered as source domains to train our network. In this paper, we report the top-1 classification accuracy on the target domains, which is averaged over three runs. We use the vanilla convolutional neural network trained on the simple aggregation of all source domains as our baseline named DeepAll.

4.2 Evaluation on PACS

Implementation Details: We use the ImageNet pretrained ResNet as our backbone. The network is trained with SGD, batch size of 16 per domain and 32 per domain for ResNet18 and ResNet50 respectively, weight decay of $1e-4$ for 6000 iterations. The c_A 's initial learning rate is 0.01, and others are 0.001, which decayed by 0.1 at every 1000 iterations. We set $\lambda = 1$, $r = 25$ and resize image to 224×224 .

Results: The results are reported in Table. 1. Our FFDI achieves the best average performance among all the compared methods including the recent methods MDGH, MixStyle, and ATSRL. On the most difficult domain Sketch has a distinct difference in data style from the remaining three domains, our performance still is almost 1.6% higher than the second-best method MDGH and also achieved satisfactory results on the remaining three domains. All the above

Target	Art	Cartoon	Photo	Sketch	Ave.
ResNet18					
DeepAll	79.6	76.0	<u>96.4</u>	66.9	79.7
MetaReg	83.7	77.2	95.5	70.3	81.7
Epi-FCR	82.1	77.0	93.9	73.0	81.5
JiGen	79.4	75.3	96.0	71.4	80.5
CrossGrad	79.8	76.8	96.0	70.2	80.7
DDAIG	84.2	78.1	95.3	74.7	83.1
CSD	78.9	75.8	94.1	76.7	81.4
L2A-OT	83.3	78.2	96.2	73.6	82.8
MixStyle	84.1	78.8	96.1	75.9	83.7
RSC	83.4	80.3	96.0	80.9	85.2
EISNet	81.9	76.4	96.0	74.3	82.2
ATSRL	85.8	80.7	97.3	77.3	85.3
MDGH	82.8	81.6	96.7	<u>81.1</u>	<u>85.5</u>
FFDI(ours)	<u>84.7</u>	<u>81.3</u>	95.5	82.7	86.0 ± 0.3
ResNet50					
DeepAll	86.3	77.6	98.2	70.1	83.0
MetaReg	87.2	79.2	97.6	70.3	83.6
CrossGrad	87.5	80.7	97.8	73.9	85.7
DDAIG	85.4	78.5	95.7	80.0	84.9
MixStyle	87.4	83.3	98.0	78.5	86.8
EISNet	86.6	81.5	97.1	78.1	85.8
RSC	87.9	82.2	97.9	<u>83.4</u>	87.8
ATSRL	90.0	<u>83.5</u>	98.9	80.0	<u>88.1</u>
MDGH	86.7	82.3	<u>98.4</u>	82.7	87.5
FFDI(ours)	<u>89.1</u>	83.9	97.2	83.7	88.5 ± 0.4

Table 1: Leave-one-domain-out results on PACS datasets with ResNet18 and ResNet50. The best results are bolded and the sub-optimal results are underlined.

Target	Art	Clipart	Product	Real Word	Ave.
DeepAll	60.3	47.8	72.7	75.0	64.0
CCSA	59.9	49.9	74.1	75.7	64.9
MMD-AAE	56.5	47.3	72.1	74.8	62.7
JiGen	53.0	47.5	71.5	72.8	61.2
CrossGrad	58.4	49.4	73.9	75.8	64.4
DDAIG	59.2	52.3	74.6	76.0	65.5
L2A-OT	60.6	50.1	<u>74.8</u>	<u>77.0</u>	65.6
MixStyle	58.7	<u>53.4</u>	74.2	75.9	65.5
ATSRL	<u>60.7</u>	52.9	75.8	77.2	66.7
FFDI(ours)	62.9	55.7	74.4	75.8	67.2 ± 0.1

Table 2: Leave-one-domain-out results on Office-Home datasets with ResNet18.

results prove that our method can significantly improve the generalization ability of the network.

4.3 Evaluation on Office-Home

Implementation Details: The network is trained with SGD, batch size of 32 per domain and weight decay of $1e-4$ for 6000 iterations. The c_A 's initial learning rate is 0.5, D , R is 0.01 and others are 0.001, which decayed by 0.1 at every 1000 iterations. We set $\lambda = 1/3$, $r = 25$ and resize image to 224×224 .

Results: The results are reported in Table. 2. Our FFDI surpasses all the comparison methods in the table. We can see that DeepAll performs well on the Office-Home dataset, which is because the image number per category is small in this dataset and the data style is similar to its pre-trained dataset ImageNet. On the two most difficult domains Art, Clipart, our performance is almost 2% higher than the second-

Target	MNIST	MNIST-M	SVHN	SYN	Ave.
DeepAll	96.6	58.1	63.7	77.9	74.1
CCSA	95.2	58.2	65.5	79.1	74.5
MMD-AAE	96.5	58.4	65.0	78.4	74.6
JiGen	96.5	61.4	63.7	74.0	73.9
CrossGrad	96.7	61.1	65.3	80.2	75.8
DDAIG	96.6	64.1	68.6	81.0	77.6
L2A-OT	96.7	63.9	68.6	83.2	78.1
MixStyle	96.5	63.5	64.7	81.2	76.5
ATSRL	97.9	62.7	69.3	83.7	78.4
FFDI(ours)	97.7	66.8	72.3	84.0	80.2 ± 0.6

Table 3: Leave-one-domain-out results on Digits-DG datasets.

best method ATSRL and MixStyle respectively. This result shows that our method can effectively improve the generalization ability of the network.

4.4 Evaluation on Digit-DG

Implementation Details: Following the experimental configuration in previous work [Zhou *et al.*, 2020b], we use the same backbone network, which is constructed by four 64 -kernels 3×3 convolution layers - ReLU - 2×2 max-pooling modules and a fully connected layer as the classifier that takes the flattened vector as input. The network is trained using SGD, batch size of 42 images per domain and weight decay of $5e-4$ for 6000 iterations. During training, our classifier’s initial learning rate is set to 0.05 and remain modules’ learning rate is 0.01, which decayed by 0.1 at every 1000 iterations. We set $\lambda = 1$, $r = 3$ and resize image to 32×32 .

Results: The results are reported in Table. 3. We can see that our approach achieves the best average performance. On the two most difficult domains, MNIST-M and SVHN, The performance of our FFDI is 8.7% and 8.6% higher than the normal model, respectively. And on the remaining two domains, MNIST and SYN, our method also obtain competitive results. This again demonstrates the effectiveness of our proposed approach.

4.5 Further Analysis

Ablation Study: We describe an ablation study to investigate the effects of different components of FFDI using PACS and ResNet18. Some of the versions used in this experiment are as follows: **H** uses only high-frequency features for classification, which is optimized by loss functions L_{ca_H} and L_{cae_H} . **L** uses only low-frequency features for classification, which is optimized by loss functions L_{ca_L} and L_{cae_L} . When we conduct interaction between **H** and **L** by using bilinear pooling, our network is optimized by using Eq. 15. **FAG** indicates frequency-domain-based data augmentation.

The results are reported in Table. 4. We can see that DeepAll achieves the best accuracy on the photo domain because it is similar to the pre-trained dataset ImageNet. When we use **H** or **L** alone, the result shows that **L** and baseline have similar performance, and **H**’s performance is better than **L** and baseline, which proves that high-frequency features can improve the generalization of the network under the encoder-decoder structure. But the improvement is not significant because of the limitations of high-frequency features. Then we introduced the feature interaction mechanism that interacts between high- and low-frequency features by using bi-

Backbone	L	H	FAG	A	C	P	S	Ave.
✓	-	-	-	79.6	76.0	96.4	66.9	79.7
✓	✓	-	-	79.1	78.0	91.1	71.9	80.0
✓	-	✓	-	81.1	77.2	93.6	73.0	81.1
✓	-	-	✓	84.1	75.1	96.6	72.2	81.9
✓	✓	✓	-	83.7	79.1	94.7	75.1	83.2
✓	✓	✓	✓	84.7	81.3	95.5	82.7	86.0

Table 4: Ablation study on PACS with ResNet18.

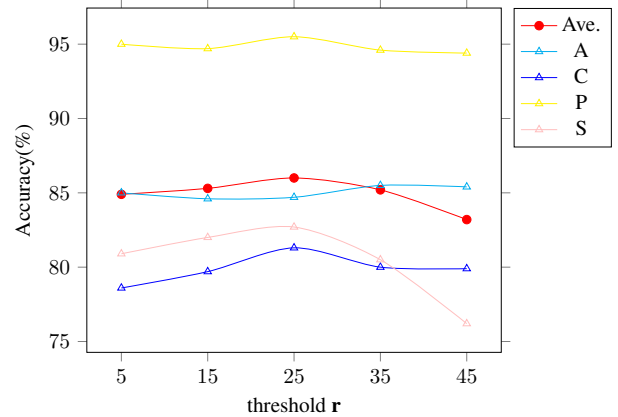


Figure 4: Experimental results for different frequency thresholds r on PACS with ResNet18.

linear pooling, which improves the accuracy by 2.1% on the **H**. This indicates that fused features can effectively enhance the representational ability of the network. **FAG** can increase the performance of baseline by 2.2%, and combining it with our proposed feature interaction method increased its performance from 83.2% to 86.0%, which shows that FAG can effectively improve the robustness of the network and plays an important role in the FFDI framework.

Impact of Different Frequency Threshold r : We report the results for art, cartoon, photo, sketch, and average performance at different frequency threshold r in Figure. 4, respectively. We find that the sketch domain is more sensitive to the value of r . As the percentage of high-frequency components decreases (as r increases), the test results in the sketch domain show a decreasing trend. The reasons for this phenomenon are due to the sketch image consisting of lines that are well described by high-frequency components. And the remaining three domains are relatively less affected by the threshold r .

5 Conclusion

In this study, we approach the domain generalization problem via frequency-specific features of the image. To address this scenario, we proposed a new method named FFDI that disentangles the high- and low-pass filtered image and then interacts between themselves to obtain the fused features that can improve the generalization ability of the model. We further introduce a simple frequency-domain-based data augmentation technology to enrich the diversity of sample distribution. Finally, we evaluated the proposed method on three benchmark datasets and reported state-of-the-art results.

References

- [Balaji *et al.*, 2018] Yogesh Balaji, Swami Sankaranarayanan, and Rama Chellappa. Metareg: Towards domain generalization using meta-regularization. In *NeurIPS*, 2018.
- [Carlucci *et al.*, 2019] Fabio M Carlucci, Antonio D’Innocente, Silvia Bucci, Barbara Caputo, and Tatiana Tommasi. Domain generalization by solving jigsaw puzzles. In *CVPR*, 2019.
- [Gonzalez-Garcia *et al.*, 2018] Abel Gonzalez-Garcia, Joost Van De Weijer, and Yoshua Bengio. Image-to-image translation for cross-domain disentanglement. In *NeurIPS*, 2018.
- [Huang *et al.*, 2020] Zeyi Huang, Haohan Wang, Eric P Xing, and Dong Huang. Self-challenging improves cross-domain generalization. In *ECCV*, 2020.
- [Huang *et al.*, 2021] Jiaxing Huang, Dayan Guan, Aoran Xiao, and Shijian Lu. Fsd: Frequency space domain randomization for domain generalization. In *CVPR*, 2021.
- [Juneja and Sandhu, 2009] Mamta Juneja and Parvinder Singh Sandhu. Performance evaluation of edge detection techniques for images in spatial domain. *IJCTE*, 2009.
- [Li *et al.*, 2017] Da Li, Yongxin Yang, Yi-Zhe Song, and Timothy M Hospedales. Deeper, broader and artier domain generalization. In *ICCV*, 2017.
- [Li *et al.*, 2018] Haoliang Li, Sinno Jialin Pan, Shiqi Wang, and Alex C Kot. Domain generalization with adversarial feature learning. In *CVPR*, 2018.
- [Li *et al.*, 2019] Da Li, Jianshu Zhang, Yongxin Yang, Cong Liu, Yi-Zhe Song, and Timothy M Hospedales. Episodic training for domain generalization. In *ICCV*, 2019.
- [Li *et al.*, 2021] Pan Li, Da Li, Wei Li, Shaogang Gong, Yanwei Fu, and Timothy M Hospedales. A simple feature augmentation for domain generalization. In *ICCV*, 2021.
- [Lin *et al.*, 2015] Tsung-Yu Lin, Aruni RoyChowdhury, and Subhransu Maji. Bilinear cnn models for fine-grained visual recognition. In *ICCV*, 2015.
- [Mahajan *et al.*, 2021] Divyat Mahajan, Shruti Tople, and Amit Sharma. Domain generalization using causal matching. In *ICML*, 2021.
- [Matsuura and Harada, 2020] Toshihiko Matsuura and Tatsuya Harada. Domain generalization using a mixture of multiple latent domains. In *AAAI*, 2020.
- [Motiian *et al.*, 2017] Saeid Motiian, Marco Piccirilli, Donald A Adjeroh, and Gianfranco Doretto. Unified deep supervised domain adaptation and generalization. In *ICCV*, 2017.
- [Peng *et al.*, 2019] Xingchao Peng, Zijun Huang, Ximeng Sun, and Kate Saenko. Domain agnostic learning with disentangled representations. In *ICML*, 2019.
- [Piratla *et al.*, 2020] Vihari Piratla, Praneeth Netrapalli, and Sunita Sarawagi. Efficient domain generalization via common-specific low-rank decomposition. In *ICML*, 2020.
- [Sanchez *et al.*, 2020] Eduardo Hugo Sanchez, Mathieu Serurier, and Mathias Ortner. Learning disentangled representations via mutual information estimation. In *ECCV*, 2020.
- [Shankar *et al.*, 2018] Shiv Shankar, Vihari Piratla, Soumen Chakrabarti, Siddhartha Chaudhuri, Preethi Jyothi, and Sunita Sarawagi. Generalizing across domains via cross-gradient training. In *ICLR*, 2018.
- [Venkateswara *et al.*, 2017] Hemant Venkateswara, Jose Eusebio, Shayok Chakraborty, and Sethuraman Panchanathan. Deep hashing network for unsupervised domain adaptation. In *CVPR*, 2017.
- [Wang *et al.*, 2020a] Guoqing Wang, Hu Han, Shiguang Shan, and Xilin Chen. Cross-domain face presentation attack detection via multi-domain disentangled representation learning. In *CVPR*, 2020.
- [Wang *et al.*, 2020b] Shujun Wang, Lequan Yu, Caizi Li, Chi-Wing Fu, and Pheng-Ann Heng. Learning from extrinsic and intrinsic supervisions for domain generalization. In *ECCV*, 2020.
- [Wang *et al.*, 2021] Jindong Wang, Cuiling Lan, Chang Liu, Yidong Ouyang, Wenjun Zeng, and Tao Qin. Generalizing to unseen domains: A survey on domain generalization. In *IJCAI*, 2021.
- [Xu *et al.*, 2021] Qinwei Xu, Ruipeng Zhang, Ya Zhang, Yanfeng Wang, and Qi Tian. A fourier-based framework for domain generalization. In *CVPR*, 2021.
- [Yang and Soatto, 2020] Yanchao Yang and Stefano Soatto. Fda: Fourier domain adaptation for semantic segmentation. In *CVPR*, 2020.
- [Yang *et al.*, 2019] Fu-En Yang, Jing-Cheng Chang, Chung-Chi Tsai, and Yu-Chiang Frank Wang. A multi-domain and multi-modal representation disentangler for cross-domain image manipulation and classification. *TIP*, 2019.
- [Yang *et al.*, 2020] Yanchao Yang, Dong Lao, Ganesh Sundaramoorthi, and Stefano Soatto. Phase consistent ecological domain adaptation. In *CVPR*, 2020.
- [Yang *et al.*, 2021] Fu-En Yang, Yuan-Chia Cheng, Zu-Yun Shiau, and Yu-Chiang Frank Wang. Adversarial teacher-student representation learning for domain generalization. In *NeurIPS*, 2021.
- [Zhou *et al.*, 2020a] Kaiyang Zhou, Yongxin Yang, Timothy Hospedales, and Tao Xiang. Deep domain-adversarial image generation for domain generalisation. In *AAAI*, 2020.
- [Zhou *et al.*, 2020b] Kaiyang Zhou, Yongxin Yang, Timothy Hospedales, and Tao Xiang. Learning to generate novel domains for domain generalization. In *ECCV*, 2020.
- [Zhou *et al.*, 2021] Kaiyang Zhou, Yongxin Yang, Yu Qiao, and Tao Xiang. Domain generalization with mixstyle. In *ICLR*, 2021.